IEICE TRANS. COMMUN., VOL.E94–B, NO.9 SEPTEMBER 2011

PAPER

Optimal Placement of Transparent Relay Stations in 802.16j Mobile Multihop Relay Networks

Yongchul KIM[†a)], ***Member and*** **Mihail L. SICHITIU**[†], ***Nonmember***

SUMMARY WiMAX (IEEE 802.16) has emerged as a promising radio access technology for providing high speed broadband connectivity to subscribers over large geographic regions. New enhancements allow deployments of relay stations (RSs) that can extend the coverage of the base station (BS), increase cell capacity, or both. In this paper, we consider the placement of transparent RSs that maximize the cell capacity. We provide a closed-form approximation for the optimal location of RS inside a cell. A numerical analysis of a number of case studies validates the closed-form approximation. The numerical results show that the closed-form approximation is reasonably accurate.

key words: *WiMAX, relay networks, optimal placement*

1. Introduction

IEEE standard 802.16, often referred to as WiMAX, is considered a "last mile" broadband wireless access alternative to conventional DSL and Cable Internet. The initial standard is focused on providing a point to multi-point (PMP) single hop service from a single base station (BS) to multiple stationary users with subscriber stations (SSs). However, several extensions have been standardized including a mesh mode, several physical layers, as well as extensions for mobility. One such extension that is recently receiving a great deal of attention is the IEEE 802.16j Mobile Multi-hop Relay (MMR) amendment. The focus of this amendment is the development of simple and lower cost relay stations (RSs) that can enhance network coverage and capacity [1].

According to the published amendment [2], RSs are classified into two categories, non-transparent mode and transparent mode. A non-transparent RS operates as a BS for connected SSs, i.e., the RS transmits management messages and forwards data traffic, while a transparent RS forwards only data traffic to and from SSs based on the frequency allocation information obtained from BS. Thus, transparent relays have to use a centralized scheduling mode. Additionally, the major difference between the two modes is that the frequency reuse is not allowed in the transparent mode. Therefore, transparent RSs are suitable for throughput improvement while non-transparent RSs are appropriate for coverage extension. We consider the placement of transparent RSs that maximize cell capacity.

There has been much research directed toward improving the capacity of wireless networks on the physical layer. However, the achievable bit rate is still limited by the received signal strength due to the fact that wireless signal attenuates severely as it propagates between transmitter and receiver. Also, in practice, there are certain intrinsic problems such as coverage holes that exist due to shadowing and the absence of line-of-sight connections, and non uniformly distributed traffic in densely populated areas. To alleviate these problems, deployment of relay stations are planned to enhance the achievable bit rate between a transmitter and a receiver leading to capacity enhancement [3].

A network operator always desires the most cost effective solution with minimal deployment expenditure for the provision of satisfactory service. Therefore, in order to provide efficient multi-hop relay networks, we need to know the optimal location of relay stations for maximizing network capacity. In this paper, we formulate optimal placements of transparent RSs that maximize the cell capacity and we also propose a closed-form approximation of optimal location of an RS in a cell. The validation section in this paper will show how accurate the approximated results are in comparison to the numerical results. By using this closed-form approximation, a network operator can easily determine where to place the RSs that maximize cell capacity with predetermined network parameters in the most practical scenarios.

The WiMAX system studied here uses an air interface based on orthogonal frequency division multiplexing (OFDM) and adaptive modulation to enhance performance when the link quality varies. The WiMAX standard supports both Time Division Duplexing (TDD) and Frequency Division Duplexing (FDD) modes, however the TDD system is of interest as it allows a flexible asymmetric Downlink (DL) to Uplink (UL) assignment ratio that is suitable for future generation wireless systems supporting multimedia services and high speed data transfers.

The balance of this paper is organized as follows. In the next section, we review related work in mobile multihop relay networks. In Sect. 3, we present the system model including terrain model, SINR analysis, fading channel, and relay strategy. In Sect. 4, we derive expressions for the optimal placement of a relay station that maximizes the mean cell capacity and the closed-form approximation solution. Numerical analysis of case studies validates the closed-form approximation in Sect. 5. Section 6 concludes the paper.

Manuscript received September 1, 2010.
Manuscript revised April 15, 2011.

[†]The authors are with the Department of Electrical and Computer Engineering, North Carolina State University, Raleigh, NC 27695, USA.
a) E-mail: yckim2@ncsu.edu

DOI: 10.1587/transcom.E94.B.2582

2. Related Work

The concept of using relays for communications has been an active research topic for more than three decades. In [4], three terminals are considered when information is transmitted over a communication channel, and an achievable lower bound to the capacity of the general relay channel is established in [5]; however, the underlying assumptions in [4], [5] are not realistic for the wireless medium. The wireless relay channel capacity was recently derived in [6]. Wireless relay channels have been considered for many applications, such as cellular networks, wireless sensor networks (WSNs), wireless local area networks (WLANs), and wireless relay/mesh networks (WMNs).

A multihop cellular network (MCN) architecture was introduced and compared with single hop cellular network (SCN) in [7]; similar to ad-hoc networks, a key feature of MCN is that mobile stations can directly communicate with each other if they are mutually reachable. The results of this work showed that MCNs can reduce the required number of base stations or improve the throughput performance by enabling a mobile station to relay data to the base station.

In [8], the problem of the optimal WSN deployment is explored with the objective of minimizing the network cost with a lifetime constraint. Additionally, the optimal number and placement of sensors that maximize the network lifetime are discussed in [9]; minimizing the energy consumption is also studied in [10].

In WLANs, extensions to the IEEE 802.11 standard were investigated to include extension points (EP) in order to improve network throughput. The study in [11] examined the optimal placement of EPs such that the throughput capacity of a rectilineal WLAN is maximized using a divide and conquer searching algorithm. For mesh networks, work in [12] focuses on minimizing the number of access points in a mesh network, while maintaining QoS constraints for all nodes.

Although related concepts have been extensively studied for various applications, there has not been much work for MMR networks. In [13], the RS deployment and relay time allocation are formulated into an optimization problem by incorporating advanced cooperative relaying technology such as decode-and-forward or compress-and-forward. The work in [14] introduced Dual-Relay MMR networks, where all the SSs are connected to the BS via two active RSs through decoded-and-forwarding scheme, and demonstrated that a Dual-Relay architecture can significantly increase network throughput. Considering the fact that WiMAX is deployed as a cellular network, [15] discussed an analytical approach for dimensioning cellular multihop WiMAX networks that are based on OFDM technology. More specifically, achievable UL and DL carrier to interference and noise ratios are examined.

In previous work, finding optimal locations of relay stations with various constraints was the main objective, however, none of those works provide a closed-form solution for the optimal placement of the RSs. In this paper, we propose a closed-form approximation and validate its performance by comparing it with numerical results. In addition, our system model is very detailed taking into account the most relevant characteristics of IEEE 802.16 systems.

3. System Model

3.1 Cellular Scenario

The considered network consists of several cells each served by a fixed central BS. A cell is divided into one to six sectors. The network is clustered in groups of four to twelve frequency channels. Each cell has a three-tiered MMR network architecture comprising a base station (BS), relay stations (RSs), and subscriber stations (SSs). The BS is responsible for providing the air interface to the SSs and is the only network entity that is connected to the backhaul network. The RSs are expected to be simple and their scheduling and resource allocation are controlled by the BS. The main responsibility of an RS is to relay data between the BS and the SSs. Although the standard allows for RS to RS connections, in this paper we assume that the SSs are at most two hops from the BS, i.e., the SSs can connect to the BS either directly or through one RS. The one-hop links between BS and RS are referred to as *relay links*, between RS and SS as *access links*, and between BS and SS as *direct links*. In addition, we assume that all nodes have a single antenna and operate in half-duplex mode and only one node can be active at a time, hence, the entire channel bandwidth is used by one node at any given time. The DL and UL channels are separated by TDD. We also assume that all channels have flat fading over one frame interval such that the channel gains remain fixed over a frame interval but change independently from one frame interval to the next. The parameters used for the analysis are listed in Table 1.

3.2 SINR Analysis

WiMAX supports a variety of modulation and coding schemes (MCS) according to channel variation. When the channel is good, a 64 QAM modulation and a 5/6 convolutional coding scheme can be applied to achieve a high data rate. For IEEE 802.16, there are 7 different physical layer data rates specified by the standard [16], denoted as $C_1, C_2, ..., C_7$. Each data rate can be realized only if the signal to interference and noise ratio (SINR) is above a certain threshold $\overline{\gamma} = \{0, \overline{\gamma}_1, \overline{\gamma}_2, ..., \overline{\gamma}_7, \infty\}$. That is, when the received SINR is in the range between $\overline{\gamma}_m$ and $\overline{\gamma}_{m+1}$, data rate C_m is achievable. The set of thresholds can be determined by a bit error rate expression for M-QAM [17]. This approximation provides a closed-form expression for the link spectral efficiency of M-QAM as a function of the SINR and bit error rate:

$$S_m = \log_2\left(1 + \frac{1.5\gamma}{-\ln 5P_b}\right), \tag{1}$$

Table 1 Simulation parameters.

System Parameters	
Operating Frequency	3.5 GHz
Duplex	TDD
Channel Bandwidth	10 MHz
BS/RS Height	50 m
SS Height	1.5 m
BS/RS Antenna Gain	17 dBi
SS Antenna Gain	0 dBi
BS/RS Power	20 W
SS Power	200 mW
BS/RS Noise Figure	3 dB
SS Noise Figure	7 dB
OFDMA Parameters	
FFT Size	1024
Sub-carrier Frequency Spacing	10.94 kHz
Useful Symbol Time	91.4 μs
Guard Time	11.4 μs
OFDM Symbol Duration	102.9 μs
Data Sub-carriers(DL/UL)	720/560
Pilot Sub-carriers(DL/UL)	120/280
Null Sub-carriers(DL/UL)	184/184
Sub-channels(DL/UL)	30/35

where S_m is the spectral efficiency, γ is SINR, and P_b is bit error rate. Table 2 shows the values of the threshold set $\overline{\gamma}$ when P_b is 10^{-6}. Accordingly, when the total channel bandwidth is used for one node, the downlink achievable data rate can be computed as:

$$C_m = \frac{3}{4}\frac{720}{102.9\,\mu\text{s}} S_m, \tag{2}$$

where 720 is the number of data sub-carriers, 102.9 μs is symbol period, and 3/4 is the downlink bandwidth share of total bandwidth. For a given transmission power P_t, the average received signal power P_r is given by:

$$P_r = \frac{G_t G_r P_t}{L}, \tag{3}$$

where G_t, G_r, and L represent the transmitting antenna gain, receiving antenna gain, and the path loss of the channel. For the path loss model, since we did not consider the mobility of the SSs in this analysis, we used the Erceg-Greenstein model [18], which is also the model recommended by the IEEE 802.16 working group for fixed wireless application system. This model was initially designed to be used in the frequency ranges close to 1.9 GHz, however, it has been expanded with a correction factor to cover higher frequency ranges from 1.9 GHz to 3.5 GHz. The basic path loss equation with the correction factor is presented in [18]:

$$\begin{aligned} L \;=\; & 20\log_{10}\left(\frac{4\pi d_0}{\lambda}\right) - 10.8\log_{10}\left(\frac{h}{2}\right) \\ & +10\alpha\log_{10}\left(\frac{d}{d_0}\right) + s + 6\log_{10}\left(\frac{f}{2000}\right), \end{aligned} \tag{4}$$

where d_0=100 m, α is the path loss exponent dependent on terrain type [18], d is the distance between the transmitter and receiver, h is the receiver antenna height, f and λ are the frequency and wavelength of the carrier signal, and

Table 2 SINR threshold set.

MCS	Downlink Data Rate C_m [Mbps]	Spectral Efficiency S_m[bps/Hz]	Threshold $\overline{\gamma}_m$ [dB]
QPSK 1/2	5.25	1.0	9.1
QPSK 3/4	7.87	1.5	11.73
16 QAM 1/2	10.49	2.0	13.87
16 QAM 3/4	15.74	3.0	17.55
64 QAM 2/3	20.99	4.0	20.86
64 QAM 3/4	23.61	4.5	22.45
64 QAM 5/6	26.23	5.0	24.02

s is a zero mean shadow fading component. The Erceg-Greenstein model has three variants, depending upon terrain type, namely A, B, and C. Type A has the highest path loss and is applicable to hilly terrains with moderate to heavy tree densities. Type C has the lowest path loss and applies to flat terrains with light tree densities. Type B is suitable for intermediate terrains. Using the propagation model, the power of the co-channel interference can also be calculated given the cluster size. Due to the assumption of a TDD synchronized network system, only co-channel SSs interfere in UL, while neighboring BSs only generate interference in DL. In the following analysis, the received SINR is determined by:

$$SINR = \frac{P_r}{P_N + \beta P_I}, \tag{5}$$

where β is the number of co-channel cells of the first tier, P_N is the noise power, P_r is the received signal power and P_I is the interference signal power from a neighboring cell on the same frequency as the current cell.

3.3 Fading Channel

In addition to the propagation model, multipath fading may have a significant effect on reliable communications. With the assumption of a Rayleigh fading channel, the received SINR, γ, is an exponential random variable [19] with the following probability density function (pdf):

$$p(\gamma) = \frac{1}{\gamma^*}\exp\left(-\frac{\gamma}{\gamma^*}\right), \gamma \geq 0, \tag{6}$$

where γ^* is the average SINR. Therefore, the probability that a transmitter can achieve data rate C_m can be expressed as:

$$p(C_m) = \int_{\overline{\gamma}_m}^{\overline{\gamma}_{m+1}} \frac{1}{\gamma^*}\exp\left(-\frac{\gamma}{\gamma^*}\right) d\gamma. \tag{7}$$

Consequently, the average achievable data rate, C_{ss}, can be computed by:

$$C_{ss} = \sum_{m=1}^{7} C_m \cdot p(C_m). \tag{8}$$

The Rician fading channel is assumed for the link between the BS and RS as RS will likely be installed within line-of-sight (LOS) of the BS. For a LOS signal, the envelope distribution of the received signal is more accurately modeled

by a Rician distribution:

$$p(\rho) = \frac{\rho}{\sigma^2} \exp\left(-\frac{\rho^2 + \nu^2}{2\sigma^2}\right) I_0\left(\frac{\rho\nu}{\sigma^2}\right), \quad (9)$$

where $I_n(\cdot)$ is the nth-order modified Bessel function of the first kind, and $\frac{1}{2}\nu^2$ and σ^2 are the power of the LOS component and the power of all other scattered components respectively. Thus, the total mean power of the received signal, Ω, can be expressed as $\Omega = \frac{1}{2}\nu^2 + \sigma^2$. The ratio between the signal power in dominant component and the local mean scattered power is defined as Rician K-factor [18], where

$$K = \frac{\nu^2}{2\sigma^2}. \quad (10)$$

When the K-factor is equal to zero, the Rician distribution becomes a Rayleigh distribution; from the pdf of received signal envelope (9), the pdf of received SINR, γ, can be derived by transforming random variable ρ into γ by considering the relationship between amplitude and power of the signal,

$$\Omega = \frac{1}{2}\rho^2. \quad (11)$$

The pdf of received SINR can be expressed as:

$$p(\gamma) = \frac{(1+K)e^{-K}}{\gamma^*} \exp\left(-\frac{(1+K)\gamma}{\gamma^*}\right) \cdot I_0\left(\sqrt{\frac{4K(1+K)\gamma}{\gamma^*}}\right), \quad (12)$$

where γ^* is the average SINR.

3.4 Relay Strategy

When RSs are deployed in a cell, the increase in cell capacity can be determined by comparing the singlehop and multihop cell capacities. We assume that an SS will use an RS to facilitate its communication with the BS only if such usage increase its expected data rate. The relay data rate (BS-RS-SS) is influenced by the link capacities of both hops involved. In order to utilize channel bandwidth efficiently, i.e., avoid wasting resource and overflowing data, the incoming and outgoing data at the relays should be equal:

$$C_{BS-RS} \cdot t_A = C_{RS-SS} \cdot t_B, \quad (13)$$

where C_{BS-RS} and C_{RS-SS} are the capacities of relay link and access link respectively when each link is given the whole bandwidth, and t_A and t_B are the durations of the relay link and access link respectively. Focusing on the DL transmission, $t_A + t_B$ should be equal to the total duration of DL frame. The frame structure for transparent RS mode can be found in [2]. The average data rate of an SS using a relay is equal to the amount of data received divided by the time required to receive it:

$$C_{BS-SS} = \frac{C_{BS-RS} \cdot t_A}{t_A + t_B}, \quad (14)$$

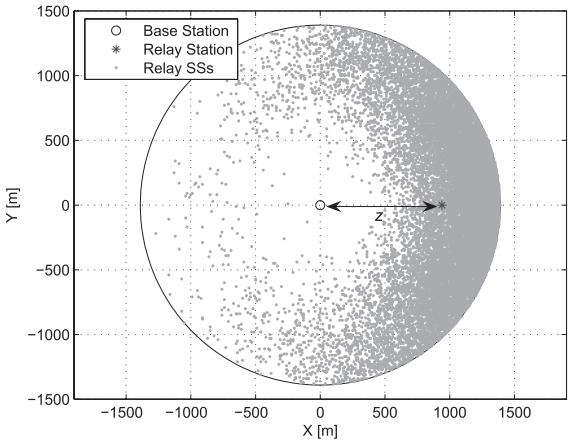

Fig. 1 A scenario with a single RS placed at distance z from the BS showing the nodes that benefit from the RS.

as the RS cannot receive from the BS while transmitting to the SS. Using (13), this can be rewritten as:

$$\frac{1}{C_{BS-SS}} = \frac{1}{C_{BS-RS}} + \frac{1}{C_{RS-SS}}. \quad (15)$$

4. Relay Location Optimization

In order to find an optimal location of RS, we need to formulate the optimization criterion. Maximizing throughput and increasing cell coverage are two different optimization objectives. To increase the cell capacity, the RS should be located well inside of BS's transmission range; on the other hand, RS should be placed close to the edge of BS's coverage to maximize the coverage of the cell. In this paper, we focus on maximizing the cell capacity and a single RS scenario is considered in order to derive an optimal placement of the RS, as we will show that it is sufficient to provide design guidelines for cells with multiple RSs.

4.1 Cell Capacity

We assume that the BS is located at the center of the cell, and the SSs are distributed uniformly in the coverage area of the BS with constant grid size. As shown in Fig. 1, the location of SS can be uniquely identified by its coordinates. Let us denote with $C_{ss}(x, y)$ the achievable data rate of an SS that is located at (x, y). The data rate $C_{ss}(x, y)$ vary according to the current SINR value. We take into account this randomness of each node's data rate when computing cell capacity. Figure 1 demonstrates that even a few SSs located on the left side of the cell are benefiting from the RS placed on the right side of the cell. If we define the set of SSs inside a cell, $\mathcal{U} = \{1, 2, ..., N\}$ where N is the total number of SSs inside a cell, the mean cell capacity can be expressed as:

$$C_{cell} = \frac{1}{N} \sum_{j \in \mathcal{U}} C_{ss}(x_j, y_j). \quad (16)$$

When a single RS is deployed in a cell, all SSs are divided

into two groups denoted as *relay SSs* and *direct SSs*. The relay SSs are benefiting from the RS as the relayed data rate is higher than direct data rate from BS. However, none of direct SSs can take advantage of the RS since the direct data rate is greater than the relay data rate. We denote with C_{ss}^{Direct} and C_{ss}^{Relay} the maximum achievable direct data rate and relay data rate of an SS respectively when the whole channel bandwidth is used for the SS. Therefore, the mean cell capacity (16) can be reformulated as:

$$C_{cell} = \frac{1}{N}\sum_{j\in\mathcal{U}} \max\left(C_{ss}^{Direct}(x_j, y_j), C_{ss}^{Relay}(x_j, y_j)\right). \quad (17)$$

By using (1) and (15), C_{ss}^{Direct} and C_{ss}^{Relay} can be expressed as:

$$C_{ss}^{Direct} = W\log_2\left(1+\frac{1.5}{-\ln 5P_b}\psi_1\gamma_1\right), \quad (18)$$

$$C_{ss}^{Relay} = W\frac{\log_2\left(1+\frac{1.5}{-\ln 5P_b}\psi_2\gamma_2\right)\cdot\log_2\left(1+\frac{1.5}{-\ln 5P_b}\psi_1\gamma_3\right)}{\log_2\left(1+\frac{1.5}{-\ln 5P_b}\psi_2\gamma_2\right)+\log_2\left(1+\frac{1.5}{-\ln 5P_b}\psi_1\gamma_3\right)},$$

where W represents the number of data sub-carriers divided by OFDM symbol duration, P_b denotes bit error rate, ψ_1 and ψ_2 are the Rayleigh and Rician fading attenuation components respectively, and the γ_1, γ_2, and γ_3 are the SINR values of BS to SS, BS to RS, and RS to SS respectively. From (3) and (5), γ_1, γ_2, and γ_3 can also be expressed as:

$$\begin{aligned}\gamma_1 &= \frac{L_I G_{BS} G_{SS} P_{BS}}{L_1(L_I P_N + \beta G_{BS} G_{SS} P_{BS})},\\ \gamma_2 &= \frac{L_I G_{BS} G_{RS} P_{BS}}{L_2(L_I P_N + \beta G_{BS} G_{RS} P_{BS})},\\ \gamma_3 &= \frac{L_I G_{RS} G_{SS} P_{RS}}{L_3(L_I P_N + \beta G_{BS} G_{SS} P_{BS})},\end{aligned} \quad (19)$$

where L_1, L_2, and L_3 are path loss values of BS to SS, BS to RS, and RS to SS respectively; L_I is the path loss of co-channel interference, G_{BS}, G_{RS}, and G_{SS} are antenna gains of BS, RS, and SS respectively, and P_{BS} and P_{RS} are transmission powers of BS and RS. When all the network parameters are known, only L_1, L_2, and L_3 are a function of the distance between the transmitter and receiver. Equation (15) shows that both C_{BS-RS} and C_{RS-SS} affect C_{ss}^{Relay}. Thus, for C_{ss}^{Relay} to be maximized both C_{BS-RS} and C_{RS-SS} should be high and approximately equal to each other. When either C_{BS-RS} or C_{RS-SS} is small, it is unlikely that C_{ss}^{Relay} is greater than C_{ss}^{Direct}.

Our objective is to find the optimal placement of the RS that maximizes the mean cell capacity. The optimal location can be determined numerically by maximizing the mean cell capacity (17) with respect to z, the distance between BS and RS. However, a closed-form solution cannot be obtained by direct differentiation. In the next subsection, we present a closed-form approximation to find the optimal placement of the RS by using approximations.

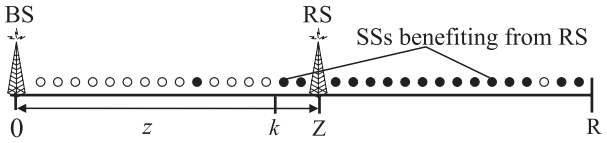

Fig. 2 A one-dimensional scenario with an RS at distance z from the BS.

4.2 Approximation

To derive a closed-form solution for the optimal location of RS, several approximations have to be made. Figure 2 shows a simplified scenario, with a BS, RS, and SSs on a one-dimensional segment. All SSs are uniformly distributed within the coverage of BS. The distance z between BS and RS represents the location of the RS, and k represents the point where C_{ss}^{Relay} is equal to C_{ss}^{Direct}:

$$C_{ss}^{Direct}(k) = C_{ss}^{Relay}(k) \quad (20)$$

Depending on the location of the RS, k can vary and can possibly be outside the cell radius R. However, it is clear that for our problem the region of interest is always within the cell since our objective is to maximize the cell capacity. When an RS is located near the BS or close to the cell edge, the locations Z and k are likely to be far away from each other, and very few SSs are benefiting from the RS. In contrast, when an RS is optimally deployed in a cell, the optimal locations Z and k are likely close to each other. Therefore, in this approximation, to facilitate the derivation, we assume that the locations of Z and k are identical. We will show that this approximation will only minimally affect the accuracy of our results.

Relay data rates of relay SSs benefiting from the RS are an important factor for maximizing cell capacity. The upper bound of cell capacity can be derived when every relay SS has a maximum relay data rate. From (15), when both relay and access link capacities are the maximum data rates, the relay data rate is maximized, i.e., the maximum relay data rate that a relay SS can achieve is half of maximum direct data rate. The achievable relay data rates of relay SSs near the RS are most likely the maximum values when the location of RS is optimal. Thus, we assume that the relay data rate, $C_{ss}^{Relay}(k)$, is always maximum value when k is at the optimal location of RS. By (18), (20) can be further simplified as:

$$\log_2\left(1+\frac{1.5}{-\ln 5P_b}\psi_1\gamma_1\right) = \frac{D}{2}, \quad (21)$$

$$\gamma_1 = \frac{L_I G_{BS} G_{SS} P_{BS}}{L_1(L_I P_N + \beta G_{BS} G_{SS} P_{BS})}, \quad (22)$$

where D is the maximum spectral efficiency that an SS can achieve within the cell. The direct link SINR γ_1 is a function of the path loss L_1 that corresponds to the optimal location of the RS. If we put (22) into (21), the path loss L_1 can be expressed as:

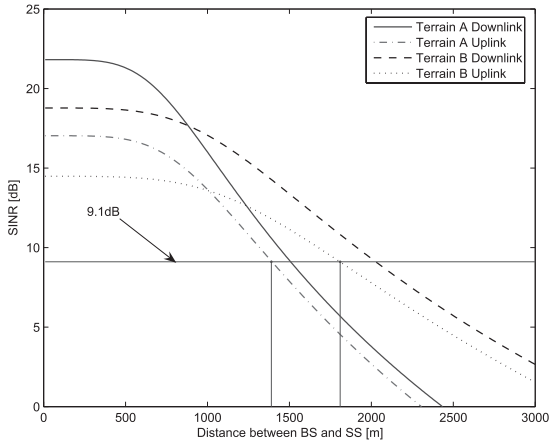

Fig. 3 Downlink and uplink edge SINR as a function of cell size for two different terrain types.

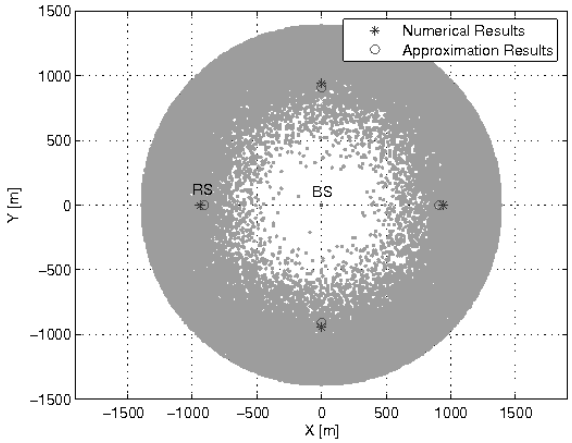

Fig. 4 Numerical results and approximation results for the basic system showing the nodes benefiting from the four RSs.

$$L_1 = \frac{1.5\psi_1 L_I G_{BS} G_{SS} P_{BS}}{(\sqrt{2^D} - 1)(-\ln 5P_b)(L_I P_N + \beta G_{BS} G_{SS} P_{BS})}. \quad (23)$$

Equation (23) can be considered as a closed-form approximation solution for optimal location of RS. Once L_1 is calculated from (23), the optimal location of RS can be easily calculated from path loss model (4).

5. Validation

In this section, the closed-form approximation is compared with the numerical solution (17) and the results are analyzed. The system is analyzed taking into account the effects of the reuse factor, sectorization, terrain type, and RS gain. Multiple RSs are also studied for a basic system. The basic system has 7 cells grouped into a cluster, one sector per cell, terrain type A, grid size 10 m, four RSs, Rician K-factor 10 dB, Rayleigh fading attenuation component −3 dB in addition to Table 1 parameters. Each of the above scenarios has a different cell size because different network parameters affect the received SINR value at the SS. We assume that the SINR values of SSs at the cell edge are greater than the minimum threshold value in Table 2, i.e., 9.1 dB. Figure 3 shows how cell size can be determined for a specific scenario. As the distance between BS and SS increases, the SINR values on both downlink and uplink decrease. In most realistic scenarios, it is more likely that the uplink SINR value is smaller than the downlink SINR due to reduced transmission power at the SSs. Once either the uplink or downlink SINR value reaches the minimum threshold value, that distance from the BS is considered as a cell size.

Figure 4 shows both the numerical results and approximated results of optimal placement for the basic system parameters. The difference between numerical value and approximated value is about 2.16% of the radius cell (i.e., 30 m). To validate the approximated result more efficiently, we define the capacity gain parameter. If C_{cell}^{Relay} and C_{cell}^{Direct} are cell capacity with RS and without RS respectively, the relative capacity gain can be defined as:

$$Capacity\ Gain = \frac{C_{cell}^{Relay} - C_{cell}^{Direct}}{C_{cell}^{Direct}}. \quad (24)$$

Therefore, the capacity gain difference between the numerical result and approximation result for the basic system case is only 0.11%. In the following subsections, we present the effect of the system parameters on the optimal placement of RS. In addition, we also evaluate the accuracy of the closed-form approximation.

5.1 Reuse Factor

The number of cells grouped in a cluster has an impact on the interference power, that is, the larger the cluster size the smaller the interference power from neighboring cells. From (3), the interference power P_I is a function of distance between co-channel cells. The co-channel distance can be expressed as $R\sqrt{3\tau}$, where τ is reuse factor, R is cell size. The cell size can also be affected by the reuse factor. The smaller the reuse factor, the smaller the cell size due to higher co-channel interference. When the cell size is small, most of the SSs do not benefit from the RSs since they are close enough to the BS leading to the smaller capacity gain. In other words, it is not desirable to deploy RSs in a smaller reuse factor case. Therefore, the reuse factors considered in this section are 7, 9, and 12. Figure 5 shows the cell capacity gain as a function of the location of RS in each reuse factor scenarios. The maximum cell capacity gain 31.54% is achieved for a reuse factor of 12. It is interesting to note that a relay is increasing the capacity of the cell even if placed near the base station due to Rayleigh fading that may result in SSs prefering the link to the RSs to the link to the BS. The differences between numerical results and the approximations of the position of the relay station are less than 6.94% (i.e., 100 m). From the cell capacity gain point of view, a 6.94% difference is negligible since cell capacity gain differences are smaller than 0.34%. The exact cell capacities and relay locations are listed in Table 3.

Table 3 Capacity and optimal relay position for the basic scenario and variations of the reuse factor, sectorization, terrain type, and RS antenna gain.

Scenario	Radius [m]	C_{cell}^{Direct} [Mbps]	Numerical Results			Approximation Results		
			Optimal Location	C_{cell}^{Relay} [Mbps]	Capacity Gain[%]	Optimal Location	C_{cell}^{Relay} [Mbps]	Capacity Gain[%]
Reuse factor 4	930	16.6132	530	18.8094	13.22	740	18.0217	8.48
Reuse factor 7	1390	12.9280	940	16.6804	29.03	910	16.6661	28.91
Reuse factor 9	1420	12.6865	980	16.5553	30.50	920	16.5346	30.33
Reuse factor 12	1440	12.5138	1020	16.4602	31.54	920	16.4186	31.20
Sector 3	1430	12.6306	1010	16.5222	30.81	920	16.4949	30.59
Sector 6	1440	12.5515	1000	16.4837	31.33	920	16.4481	31.04
Terrain B	1810	12.4314	1110	16.1237	29.70	1150	16.1193	29.67
Terrain C	2120	12.2409	1250	15.7743	28.87	1320	15.7068	28.31
RS Gain 10 dB	1390	12.9272	940	15.7502	21.84	910	15.7474	21.82
RS Gain 5 dB	1390	12.9266	890	14.7527	14.13	910	14.7449	14.07

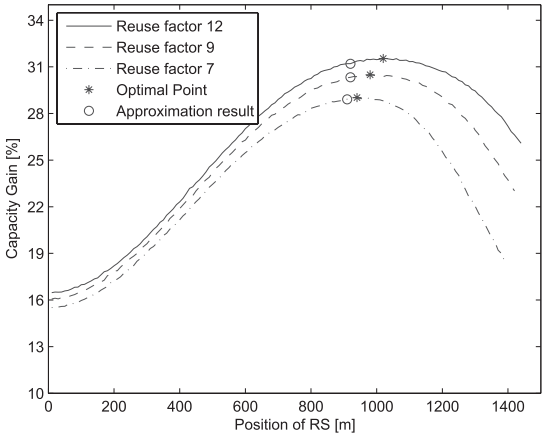

Fig. 5 Cell capacity gain as a function of the position of the relay station for different reuse factors.

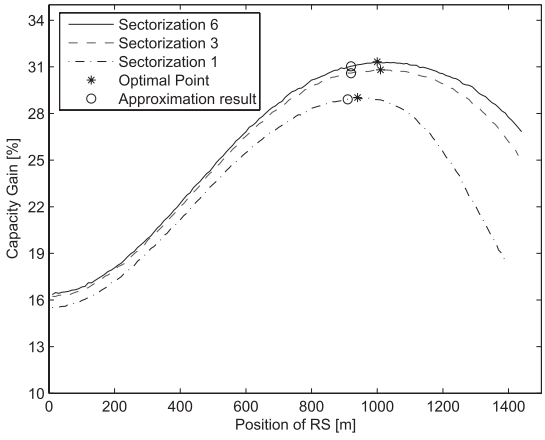

Fig. 6 Cell capacity gain as a function of the position of the relay station for different sectorizations.

5.2 Sectorization

We study different sectorization scenarios for the basic system parameters. Sectorization is normally used to increase cell capacity by replacing the omni-directional antenna at each BS with three or six sector antennas. Each sector can be considered as a new cell with its own frequency channels. The use of sector antennas reduces the number of co-channel interferences. For example, when three sector antennas are used in a cell, the number of co-channel interferences is reduced from 6 to 2. Figure 6 shows the effect of sectorization on the optimal placement of RSs as well as the differences between numerical results and approximated results. It is obvious that the higher the number of sectors the higher the capacity gain. The distances between optimal points from numerical results and approximation results are less than 6.25% (i.e., 90 m) and the corresponding cell capacity gain differences are less than 0.29%.

5.3 Terrain Types

Terrain types mentioned in Sect. 3.2 are studied in this subsection to validate the closed-form approximation results with numerical results. Since terrain type A has the highest path loss, the cell size will be the smallest (at 1390 m), while terrain type C has the lowest path loss and the largest cell size (at 2120 m). Figure 7 shows achievable capacity gains with respect to the location of RS for different terrain type scenarios. The ratio of optimal location of RS to each cell radius is decreasing as terrain type is changing from A

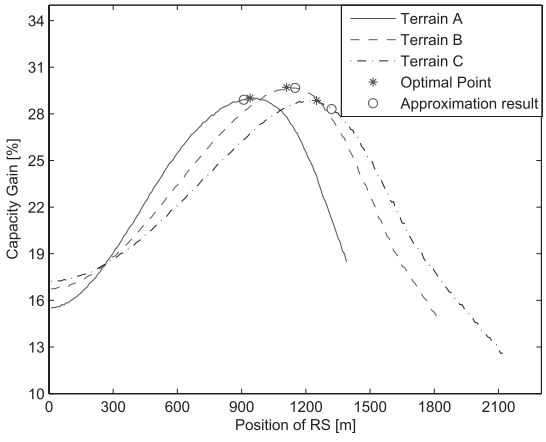

Fig. 7 Cell capacity gain as a function of the position of the relay station for different terrain types.

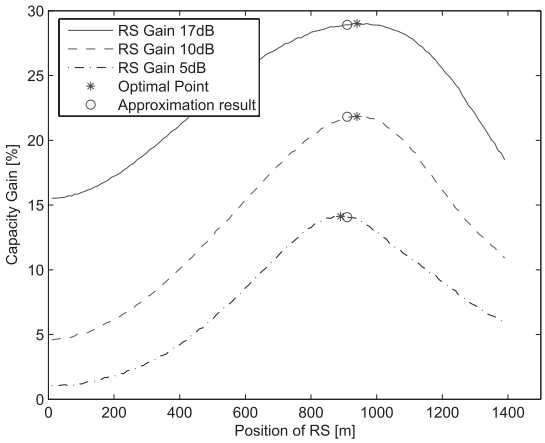

Fig. 8 Cell capacity gain as a function of the position of the relay station for different RS antenna gains.

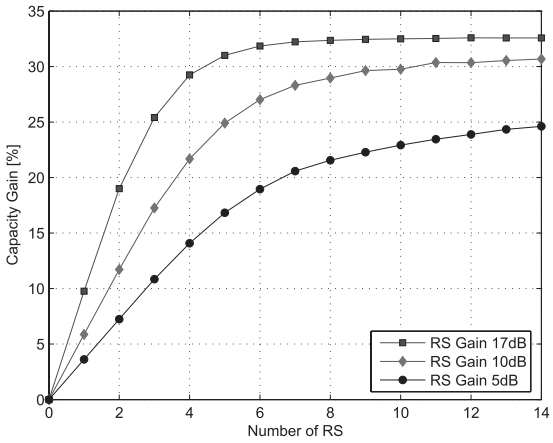

Fig. 9 Cell capacity gain as a function of number of RS for different RS antenna gains.

to C. When terrain type is A, the optimal location of RS is 67.63% of the cell radius, while optimal location of RS for terrain type C is 58.96%. However, the maximum capacity gains for each scenario are very similar to each other, 29.7% is achieved for terrain type B and 28.87% is achieved for terrain type C. The distances between optimal points from numerical results and approximation results are less than 3.3% (i.e., 70 m) and the corresponding cell capacity gain differences are less than 0.56%.

5.4 RS Antenna Gain

From the basic system parameters listed in Table 1, the RS antenna gain is 17 dBi as same as BS antenna gain. We study how RS antenna gain can affect the optimal placement of the RS and cell capacity by varying the antenna gain of the RS. Although RSs are expected to be less expensive to deploy than a BS, the antenna gain of RS does not always have to be lower than BS antenna gain. Figure 8 shows that the lower the RS antenna gain the lower the capacity gain achieved. It is also shown that the different antenna gains of RS had no significant impact on the optimal placement of RS, but the achievable capacity gain differences are nearly proportional to the antenna gain of RS. The maximum capacity gain is 29.03% when RS gain is 17 dBi and the lowest capacity gain is 14.13% when RS gain is 5 dBi. The capacity gain differences between numerical results and approximation results are exceedingly small in all cases. The largest difference is only 0.12% when the RS gain is 17 dBi.

5.5 Multiple RSs

As shown in Fig. 4, multiple RSs can be used to increase the capacity gain. Considering the objective of minimizing the network cost, it is worthwhile to know how many RSs would be appropriate to maximize cell capacity gain. Figure 9 shows how much capacity gain can be achieved with respect to the number of RS when the RSs are arranged in a circular pattern at the optimal distance from the BS. When the RS antenna gain is 17 dBi, capacity gain is almost linearly increasing until the number of RS is three, and after that the increase of capacity gain is diminishing as the number of RS is growing. Therefore, there is no use to deploy more than six RSs in this particular network scenario. When the RS antenna gains are 10 dBi and 5 dBi, the capacity gains converge around 31% and 25% respectively. A cell may include any number of relay stations of antenna gain of 5 dBi, but the achievable capacity gain is less than that of a system with five RSs of antenna gain 10 dBi or three RSs of antenna gain 17 dBi. In order to maximize the cell capacity gain, RS antenna gain is more important than the number of RSs.

5.6 Outage Probability

Addition of RSs can significantly reduce the outage probability of communication systems. The outage probability is defined as the probability that the instantaneous received SINR is below a minimum threshold value. The direct path (BS-SS) outage probability can be expressed as:

$$P_{out}(Direct\ path) = p\left(\gamma_1 < \overline{\gamma}_{min}\right), \tag{25}$$

where γ_1 is the SINR value of BS to SS and $\overline{\gamma}_{min}$ is the minimum threshold SINR value. When a single RS is placed at the optimal location, the relay path (BS-RS-SS) outage probability can be computed by:

$$P_{out}\left(Relay\ path\right) = 1 - \{p\left(\gamma_2 > \overline{\gamma}_{min}\right) \cdot p\left(\gamma_3 > \overline{\gamma}_{min}\right)\}, \tag{26}$$

where γ_2 and γ_3 are SINR values of BS to RS and RS to SS. Due to the fact that BS can opportunistically choose better communication channel between the direct path and relay path, the transmission will fail only if both direct and relay link fail simultaneously. Therefore, the outage probability of using RS is $P_{out} = P_{out}(Direct\ path) \times P_{out}(Relay\ path)$. As shown in Fig. 10, the outage probability of using RS is significantly reduced at all positions. The largest outage probability is around 50% in the direct path case, while it

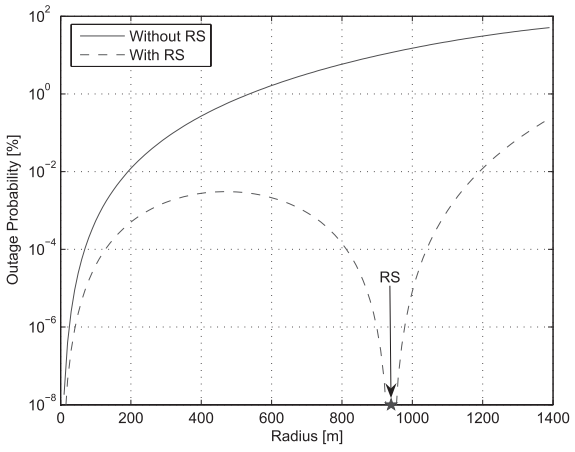

Fig. 10 Outage probability as a function of distance from BS with and without an RS.

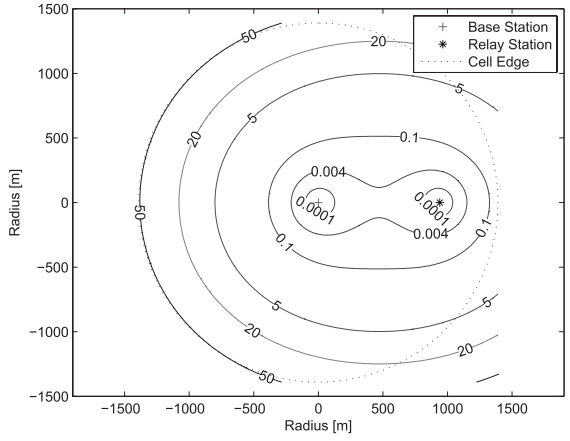

Fig. 11 Outage probability contour graph with a single RS.

is only 0.11% when an RS is used. Figure 11 shows contour plot of outage probability when a single RS is optimally placed inside a cell.

6. Conclusion

This paper presents the optimal placement of RS in MMR networks. The results show how various network parameters such as reuse factor, sectorization, terrain type, number of RSs, and their antenna gain affect the optimal placements of RSs. The main contribution of this work is presenting an accurate model for the cell capacity of 802.16 MMR systems. We also present a closed-form approximation for the optimal placement of an RS. The closed-form expression can be used by network designers to compute the optimal placements of RSs in most practical cases. From the numerical analysis, we have shown that approximation results from closed-form are reasonably accurate.

References

[1] J. Sydir, "Harmonized contribution 802.16j (Mobile Multihop Relay) usage models," http://grouper.ieee.org/groups/802/16/relay/docs/80216j-06-015.pdf, 2006.

[2] "IEEE Std 802.16j, amendment to IEEE standard for local and metropolitan area networks," 2009.

[3] N. Esseling, B. Walke, and R. Pabst, Fixed Relays For Next Generation Wirelss Systems, Springer Science+Buisness Media, New York, USA, 2005.

[4] E.C.V.D. Meulen, "Three-terminal communication channels," Adv. Appl. Probab., vol.3, no.1, pp.120–154, 1971.

[5] T. Cover and A. Gamal, "Capacity theorems for the relay channel," IEEE Trans. Inf. Theory, vol.25, no.5, pp.572–584, Sept. 1979.

[6] A. Host-Madsen and J. Zhang, "Capacity bounds and power allocation for wireless relay channels," IEEE Trans. Inf. Theory, vol.51, no.6, pp.2020–2040, June 2005.

[7] Y.D. Lin and Y.C. Hsu, "Multihop cellular: a new architecture for wireless communications," Proc. IEEE INFOCOM. Nineteenth Annual Joint Conference of the IEEE Computer and Communications Societies, vol.3, pp.1273–1282, March 2000.

[8] K. Xu, Q. Wang, H. Hassanein, and G. Takahara, "Optimal wireless sensor networks (WSNs) deployment: Minimum cost with lifetime constraint," Proc. IEEE International Conference on Wireless And Mobile Computing, Networking And Communications (WiMob), vol.3, pp.454–461, Aug 2005.

[9] Y. Chen, C.N. Chuah, and Q. Zhao, "Sensor placement for maximizing lifetime per unit cost in wireless sensor networks," Military Communications Conference, vol.2, pp.1097–1102, Oct. 2005.

[10] M. Patel, R. Chandrasekaran, and S. Venkatesan, "Energy efficient sensor, relay and base station placements for coverage, connectivity and routing," Proc. 24th IEEE International Conference on Performance, Computing, and Communications (IPCCC), pp.581–586, April 2005.

[11] A. So and B. Liang, "An efficient algorithm for the optimal placement of wireless extension points in rectilineal wireless Local Area Networks," Proc. International Conference on Quality of Service in Heterogeneous Wired/Wireless Networks, p.25, 2005.

[12] Y. Bejerano, "Efficient integration of multi-hop wireless and wired networks with QoS constraints," Proc. International Conference on Mobile Computing and Networking (MobiCom), pp.215–226, ACM, 2002.

[13] B. Lin, P.H. Ho, L.L. Xie, and X. Shen, "Optimal relay station placement in IEEE 802.16j networks," Proc. International Conference on Wireless Communications and Mobile Computing (IWCMC), pp.25–30, Aug. 2007.

[14] B. Lin, P.H. Ho, L.L. Xie, and X. Shen, "Relay station placement in IEEE 802.16j Dual-Relay MMR Networks," Proc. IEEE International Conference on Communications (ICC), pp.3437–3441, May 2008.

[15] C. Hoymann, M. Dittrich, and S. Goebbels, "Dimensioning cellular multihop WiMAX networks," IEEE Mobile WiMAX Symposium, pp.150–157, 2007.

[16] J.G. Andrews, A. Ghosh, and R. Muhamed, Fundamentals of WiMAX: Understanding Broadband Wireless Networking, Prentice Hall PTR, Upper Saddle River, NJ, USA, 2007.

[17] G.J. Foschini and J. Salz, "Digital communications over fading radio channels," Bell Syst. Tech. J., pp.429–456, Feb. 1983.

[18] V. Erceg and K.V.S. Hari, "Channel models for fixed wireless applications," IEEE 802.16 Broadband Wireless Access Working Group, Technical Report, 2001.

[19] Q. Zhang and S. Kassam, "Finite-state markov model for Rayleigh fading channels," IEEE Trans. Commun., vol.47, no.11, pp.1688–1692, Nov. 1999.

Yongchul Kim was bone in Sungnam, South Korea. He received a B.E. from Korea Military Academy in 1998 and an M.S. from the university of Surrey (Surrey, UK) in 2001. He was a full time instructor in Korea Military Academy until 2007 and he is currently a Ph.D. candidate at the North Carolina State University (Raleigh, USA) with research interests in wireless networking and WiMAX.

Mihail L. Sichitiu born in Bucharest, Romania. He received a B.E. and an M.S. in Electrical Engineering from the Polytechnic University of Bucharest in 1995 and 1996 respectively. In May 2001, he received a Ph.D. degree in Electrical Engineering from the University of Notre Dame. He is currently employed as an associate professor in the Department of Electrical and Computer Engineering at North Carolina State University. His primary research interest is in Wireless Networking with emphasis on multi-hop networking and wireless local area networks.